

# A Novel 700 V Monolithically Integrated Si-GaN Cascoded Field Effect Transistor

Jie Ren<sup>ID</sup>, Student Member, IEEE, Chak Wah Tang, Hao Feng, Huaxing Jiang<sup>ID</sup>, Member, IEEE,  
Wentao Yang<sup>ID</sup>, Student Member, IEEE, Xianda Zhou, Member, IEEE,  
Kei May Lau, Fellow, IEEE, and Johnny K. O. Sin, Fellow, IEEE

**Abstract**—In this letter, a novel monolithically integrated Si-GaN cascaded FET is designed and experimentally demonstrated for high-voltage power switching applications. The device is formed by monolithically connecting a low-voltage Si MOSFET and a high-voltage normally-on GaN MIS-HEMT on the same substrate in the cascode configuration. The interconnection distance is  $50\ \mu\text{m}$  which is only 2.5% of that of the conventional two-chip co-package approach ( $\sim 2\ \text{mm}$ ). The fabricated cascaded FET features normally-off functionalities with a threshold voltage of 3.2 V, a drive current of  $1850\ \text{A/cm}^2$  ( $630\ \text{mA/mm}$ ) at the gate bias of 15 V, a gate swing of 20 V, a specific on-resistance of  $3.3\ \text{m}\Omega\cdot\text{cm}^2$  and a breakdown voltage of 696 V.

**Index Terms**—Monolithic integration, cascade configuration, power FETs, GaN, MIS-HEMT, power switching electronics.

## I. INTRODUCTION

GaN-BASED power devices are promising candidates for power electronic applications due to the superior material properties of GaN compared with those of Si. But there are still obstacles keeping GaN transistors from dominating the market. The common disadvantages are the normally-on characteristics, low positive threshold voltage of Enhancement-mode devices [1], large gate leakage current, small gate voltage swing [2], and large reverse voltage drop [3]. Although some approaches were proposed to overcome one or some of the above obstacles [4], [5], it is extremely difficult to resolve these problems without sacrificing the overall performance. A hybrid Si-GaN cascode approach is the simplest solution to the above problems up to now and has been adopted by the commercial sector [6]. However, the conventional

Manuscript received November 29, 2017; revised January 4, 2018; accepted January 7, 2018. Date of publication January 10, 2018; date of current version February 22, 2018. This work was supported in part by the Research Grants Council of Hong Kong under the General Research Fund under Grant 16212415 and Grant T23-612/12-R, and in part by the Introduction of Innovative Research and Development Team project. The review of this letter was arranged by Editor T. Palacios. (Corresponding author: Jie Ren.)

J. Ren, C. W. Tang, H. Feng, H. Jiang, W. Yang, K. M. Lau, and J. K. O. Sin are with the Department of Electronic and Computer Engineering, The Hong Kong University of Science and Technology, Hong Kong (e-mail: jrenab@connect.ust.hk).

X. Zhou is with the School of Electronics and Information Technology, Sun Yat-Sen University, Guangzhou 510006, China.

Color versions of one or more of the figures in this letter are available online at <http://ieeexplore.ieee.org>.

Digital Object Identifier 10.1109/LED.2018.2791586

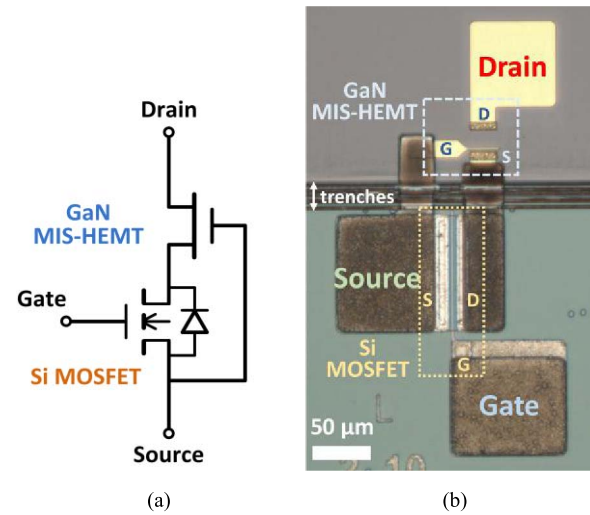


Fig. 1. (a) Circuit schematic of the cascaded FET, and (b) a top view image of the fabricated cascaded FET.

Si-GaN cascode configuration is achieved by using the two-chip co-package approach which features a long interconnection distance between the Si and GaN devices. The large interconnection parasitics induced by bonding wires will cause undesirable ringing during fast switching, resulting in lower system stability and higher switching losses [7]. One efficient way to minimize the parasitics is to fully integrate the Si MOSFET and GaN MIS-HEMT on the same substrate with a short interconnection distance. In doing so, the overall package size and assembly costs can also be reduced.

In this letter, the fabrication technology for integrating the low-voltage Si MOSFET and high-voltage GaN MIS-HEMT on the same Si substrate is developed. A Si-GaN cascaded FET is demonstrated using this technology with an interconnection distance of  $50\ \mu\text{m}$  which is less than 3% of that of the conventional two-chip co-package approach ( $\sim 2\ \text{mm}$  bonding wires).

## II. DEVICE STRUCTURE AND FABRICATION

The schematic of the Si-GaN cascaded FET equivalent circuit is shown in Fig. 1(a), which consists of a low-voltage normally-off Si MOSFET and a high-voltage normally-on GaN MIS-HEMT. For turning on of the cascaded FET,

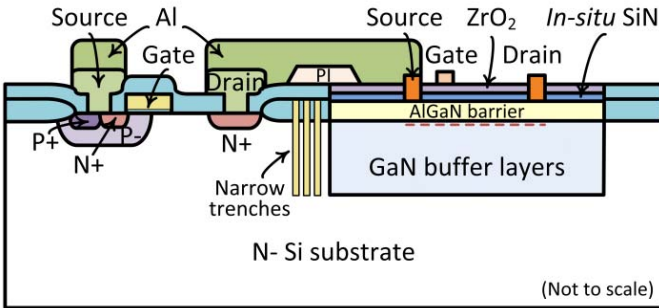


Fig. 2. Schematic cross-sectional view of the cascaded FET.

a positive voltage is applied to the gate electrode. The drain-to-source voltage of the Si MOSFET ( $V_{DS,Si}$ ) will then decrease, and the gate-to-source voltage of the GaN MIS-HEMT ( $V_{GS,GaN}$ ) will increase accordingly. When  $V_{GS,GaN}$  is larger than the threshold voltage of the GaN MIS-HEMT ( $V_{th,GaN}$ ), the MIS-HEMT is turned on with high current/power capability. In the on-state, the total on-resistance is the sum of the Si MOSFET and GaN MIS-HEMT. For the device turn-off, the gate voltage is removed and the Si MOSFET is turned off with an increase in  $V_{DS,Si}$  and decrease in  $V_{GS,GaN}$  accordingly. When the  $V_{GS,GaN}$  is lower than the  $V_{th,GaN}$ , the GaN MIS-HEMT is turned off with high-voltage blocking capability. During the reverse conduction, the gate and source are connected to the ground, then the body diode of the Si MOSFET and the GaN MIS-HEMT form a cascaded diode which will conduct the reverse current with a small voltage drop [8].

A top view image of the fabricated cascaded FET is shown in Fig. 1 (b). It can be seen that the Si and GaN devices are placed on the same substrate with a distance of 50  $\mu\text{m}$ . Cross-sectional view of the cascaded FET is shown in Fig. 2. The monolithic integration technology used for the cascaded FET fabrication is from the continued development of the cascaded diode [8]. The process begins with a 4-inch n- Si (111) wafer. The Si devices are isolated by LOCOS. Besides, the Si and GaN device regions are isolated by etched narrow trenches. Then the approximately 4  $\mu\text{m}$  AlGaN/GaN epitaxial layers with 8 nm *in-situ* SiN are grown in the Si recessed windows by MOCVD selective epitaxial growth (SEG). A near planar configuration of the GaN and Si device surface is achieved, which is important for fine-pattern lithography. Subsequently, the Si laterally diffused MOSFET processes are carried out, including poly Si gate etching and junction formation. During the high-temperature drive-in step of the p-body region,  $\text{SiO}_2$  is used to cover the GaN epitaxial layers to protect the surface from decomposition [9]. After that, the GaN MIS-HEMT is processed with argon implantation isolation. And the *in-situ* SiN and 19 nm of ALD  $\text{ZrO}_2$  are used as the gate dielectrics [10]. Finally, the Si and GaN devices are connected by Al metal lines.

### III. EXPERIMENTAL RESULTS AND DISCUSSION

In the fabricated cascaded FET, the active area of the Si MOSFET is 300  $\mu\text{m}^2$ , where the poly Si gate length, gate-to-drain distance and gate width are 2  $\mu\text{m}$ , 1  $\mu\text{m}$  and 100  $\mu\text{m}$ ,

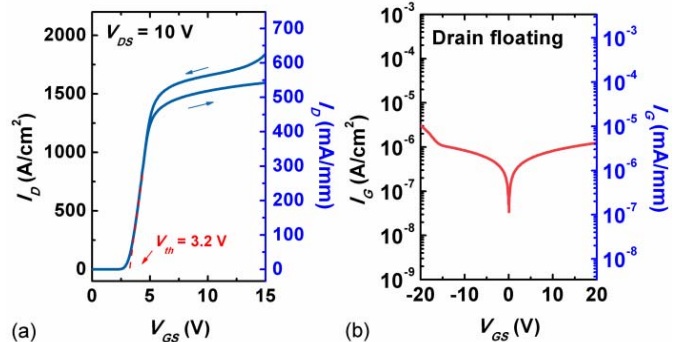


Fig. 3. (a) DC  $I_D$ - $V_{GS}$  characteristics of the cascaded FET with the gate bias down/up sweeping at a drain bias of 10 V, and (b) DC  $I_G$ - $V_{GS}$  characteristics of the cascaded FET with drain electrode floating.

respectively. The active area of the GaN MIS-HEMT is 380  $\mu\text{m}^2$ , with a gate length of 2  $\mu\text{m}$ , gate-to-source distance of 2  $\mu\text{m}$ , gate-to-drain distance ( $L_{GD,GaN}$ ) of 15  $\mu\text{m}$ , and gate width of 20  $\mu\text{m}$ . The interconnection distance between the Si MOSFET and GaN MIS-HEMT is 50  $\mu\text{m}$ .

Fig. 3 (a) shows the dc transfer characteristics of the Si-GaN cascaded FET, which have been normalized to the total active area (680  $\mu\text{m}^2$ , the sum of the active area of the Si MOSFET and the GaN MIS-HEMT), and the gate width of the MIS-HEMT ( $W_{GaN}$ , 20  $\mu\text{m}$ ) as represented by the left axis and right axis, respectively. The  $V_{th}$  determined by the linear extrapolation method is extracted to be 3.2 V. Furthermore, as shown in Fig. 3 (b), a large gate swing of 20 V is measured. At the  $V_{GS}$  of  $\pm 20$  V, the gate leakage current is smaller than  $10^{-5}$  mA/mm, which is difficult to achieve in GaN-based transistors. Such a high  $V_{th}$  and large gate swing are important for preventing the faulty turn-on by electromagnetic interference and make the cascaded FET compatible with the existing gate drive circuits designed for Si-based power transistors [11]. The current on/off ratio is measured to be  $2 \times 10^8$ . The transfer curve is obtained using double sweeping mode at  $V_{DS}$  of 10 V, and no  $V_{th}$  shift is observed when the  $V_{GS}$  sweeps from 15 V down to 0 V and from 0 V up to 15 V. It indicates a very good interface quality of the Si MOSFET. The double sweep  $I_D$ - $V_{GS}$  characteristics show approximately 10 % discrepancy in  $I_D$  at  $V_{GS}$  larger than 5 V. This is due to the unoptimized surface passivation of the GaN MIS-HEMT, which can be further improved by combining additional PECVD SiN passivation [12].

The dc output characteristics of the cascaded FET are shown in Fig. 4. The dc specific on-resistance ( $R_{on,sp}$ ) is extracted as 3.3  $\text{m}\Omega \cdot \text{cm}^2$  (on-resistance normalized to total active area), and 9.7  $\Omega \cdot \text{mm}$  (on-resistance normalized to  $W_{GaN}$ ) at a gate bias of 15 V. The device exhibits a drive current of 1850 A/ $\text{cm}^2$  (normalized to total active area) and 630 mA/mm (normalized to  $W_{GaN}$ ). In the saturation region of the output curve with the gate bias of 15 V, the  $V_{GS,GaN}$  is measured to be -1.5 V. The GaN MIS-HEMT with  $V_{th,GaN}$  of -7 V has a gate overdrive voltage of 5.5 V. This ensures the higher drive current (630 mA/mm) of the cascaded FET compared with the normally-off GaN FETs [1]-[5], [13].

During the off-state breakdown test, the gate and source electrodes are grounded with the substrate floating.

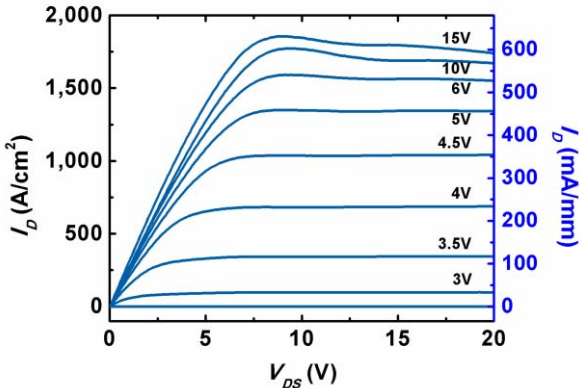


Fig. 4. DC  $I_D$ - $V_D$  characteristics of the cascaded FET.

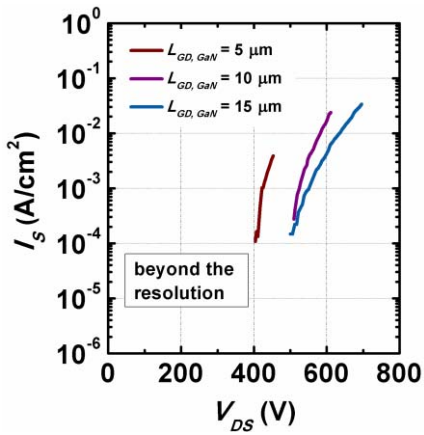


Fig. 5. Off-state I-V characteristics of the fabricated cascaded FETs with various  $L_{GD,GaN}$ .

When  $V_{DS}$  increases, the Si MOSFET is driven into avalanche breakdown due to the high leakage current from the source of the GaN MIS-HEMT. The cascaded FET continues blocking the increased reverse voltage by the GaN MIS-HEMT with the Si MOSFET in avalanche mode. A resistor or a Zener diode in parallel with the Si MOSFET can improve the device reliability in the off-state [14]. Due to the good leakage suppression of the Si MOS gate structure, the gate current of the cascaded FET is negligible compared with the source and drain leakage current. The off-state source current of the cascaded FETs with various GaN MIS-HEMTs dimensions are measured by Tektronix 370A and plotted in Fig. 5.  $V_{BD}$  of the cascaded FETs with  $L_{GD,GaN}$  of 5  $\mu\text{m}$ , 10  $\mu\text{m}$ , and 15  $\mu\text{m}$  are 453 V, 611 V and 696 V, respectively. For the device with  $L_{GD,GaN}$  of 15  $\mu\text{m}$ , the source leakage current is 0.034 A/cm<sup>2</sup> at the breakdown point, which is equal to 0.01 mA/mm when normalized to  $W_{GaN}$ . At 500 V, the source leakage current is approximately 0.1 mA/cm<sup>2</sup> (0.03  $\mu\text{A}/\text{mm}$ ), which is comparable with the state-of-art normally-off GaN-based MIS (MOS)-HEMTs [5], [13].

#### IV. CONCLUSION

In conclusion, a Si-GaN cascaded FET has been demonstrated using the monolithic integration technology. The device features an on-chip interconnection distance of 50  $\mu\text{m}$ ,

a threshold voltage of 3.2 V, a gate swing of 20 V, a specific on-resistance of 3.3  $\text{m}\Omega \cdot \text{cm}^2$  and a breakdown voltage of 696 V. Furthermore, the technology provides the foundation to explore the fully integration of III-Nitride compound semiconductor devices/circuits with Si devices/circuits for power electronic applications.

#### ACKNOWLEDGMENT

The authors would like to thank the staff of the Nanosystem Fabrication Facility, Photonics Technology Center, and the Semiconductor Product Analysis and Design Enhancement Center, the Hong Kong University of Science and Technology, for their help in device fabrication and characterization.

#### REFERENCES

- [1] W. Saito, Y. Takada, M. Kuraguchi, K. Tsuda, and I. Omura, "Recessed-gate structure approach toward normally off high-voltage AlGaN/GaN HEMT for power electronics applications," *IEEE Trans. Electron Devices*, vol. 53, no. 2, pp. 356–362, Feb. 2006, doi: [10.1109/TED.2005.862708](https://doi.org/10.1109/TED.2005.862708).
- [2] Y. Uemoto, M. Hikita, H. Ueno, H. Matsuo, H. Ishida, M. Yanagihara, T. Ueda, T. Tanaka, and D. Ueda, "Gate injection transistor (GIT)—A normally-off AlGaN/GaN power transistor using conductivity modulation," *IEEE Trans. Electron Devices*, vol. 54, no. 12, pp. 3393–3399, Dec. 2007, doi: [10.1109/TED.2007.908601](https://doi.org/10.1109/TED.2007.908601).
- [3] O. Hilt, A. Knauer, F. Brunner, E. Bahat-Treidel, and J. Würfl, "Normally-off AlGaN/GaN HFET with p-type Ga gate and AlGaN buffer," in *Proc. IEEE 22nd Int. Symp. Power Semiconductor Devices ICs (ISPSD)*, Hiroshima, Japan, Jun. 2010, pp. 347–350.
- [4] T. Oka and T. Nozawa, "AlGaN/GaN recessed MIS-gate HFET with high-threshold-voltage normally-off operation for power electronics applications," *IEEE Electron Device Lett.*, vol. 29, no. 7, pp. 668–670, Jul. 2008, doi: [10.1109/LED.2008.2000607](https://doi.org/10.1109/LED.2008.2000607).
- [5] Z. Tang, Q. Jiang, Y. Lu, S. Huang, S. Yang, X. Tang, and K. J. Chen, "600-V normally off Si<sub>x</sub>/AlGaN/GaN MIS-HEMT with large gate swing and low current collapse," *IEEE Electron Device Lett.*, vol. 34, no. 11, pp. 1373–1375, Nov. 2013, doi: [10.1109/LED.2013.2279846](https://doi.org/10.1109/LED.2013.2279846).
- [6] Transphorm, Goleta, CA, USA. *TPH3202LS Datasheet*. Accessed: 2017. [Online]. Available: <http://www.transphormusa.com>
- [7] Z. Liu, X. Huang, F. C. Lee, and Q. Li, "Package parasitic inductance extraction and simulation model development for the high-voltage cascode GaN HEMT," *IEEE Trans. Power Electron.*, vol. 29, no. 4, pp. 1977–1985, Apr. 2014, doi: [10.1109/TPEL.2013.2264941](https://doi.org/10.1109/TPEL.2013.2264941).
- [8] J. Ren, C. Liu, C. W. Tang, K. M. Lau, and J. K. O. Sin, "A novel Si-GaN monolithic integration technology for a high-voltage cascaded diode," *IEEE Electron Device Lett.*, vol. 38, no. 4, pp. 501–504, Apr. 2017, doi: [10.1109/LED.2017.2665698](https://doi.org/10.1109/LED.2017.2665698).
- [9] J. Ren, C. Liu, K. M. Lau, and J. K. O. Sin, "Effects of high-temperature thermal treatment on AlGaN/GaN HEMT Epi for monolithic integration," presented at the Int. Conf. Nitride Semiconductors (ICNS), Beijing, China, Aug./Sep. 2015, Paper A0399.
- [10] H. Jiang, C. Liu, Y. Chen, C. W. Tang, and K. M. Lau, "Low leakage high breakdown GaN MOSHEMTs on Si with a ZrO<sub>2</sub> gate dielectric," in *Proc. CS ManTech Conf.*, Indian Wells, CA, USA, May 2017, pp. 1–4.
- [11] E. Persson, "Practical application of 600 V GaN HEMTs in power electronics," presented at the IEEE APEC Professional Edu. Seminar S17, Charlotte, NC, USA, 2015.
- [12] H. Jiang, C. Liu, Y. Chen, X. Lu, C. W. Tang, and K. M. Lau, "Investigation of *in situ* SiN as gate dielectric and surface passivation for GaN MISHEMTs," *IEEE Trans. Electron Devices*, vol. 64, no. 3, pp. 832–839, Jan. 2017, doi: [10.1109/TED.2016.2638855](https://doi.org/10.1109/TED.2016.2638855).
- [13] J. J. Freedman, T. Egawa, Y. Yamaoka, Y. Yano, A. Ubukata, T. Tabuchi, and K. Matsumoto, "Normally-off Al<sub>2</sub>O<sub>3</sub>/AlGaN/GaN MOS-HEMT on 8 in. Si with low leakage current and high breakdown voltage (825 V)," *Appl. Phys. Exp.*, vol. 7, no. 4, p. 041003, Apr. 2014, doi: [10.7567/APEX.7.041003](https://doi.org/10.7567/APEX.7.041003).
- [14] R. K. Lal, R. Coffie, Y. Wu, P. Parikh, Y. Dora, U. Mishra, S. Chowdhury, and N. Fichtenbaum, "High power semiconductor electronic components with increased reliability," U.S. Patent 8598937 B2, Dec. 3, 2015.